Transfer Station Analysis

Andrew I. Hustrulid, PhD[1]

The discrete element method has successfully been used to model the behavior of material flow in transfer stations. With position, velocity, and applied forces for every particle and boundary in the simulation available at increments of 10^{-5} seconds, the next critical step is the presentation of this data in a concise and beneficial form. This paper discusses several methods of presenting the data from discrete element simulations that are used to improve the performance of a transfer station. These measurements are also used as a learning tool to better understand and visualize how material transfers from one belt to the next.

THE DISCRETE ELEMENT METHOD

The Discrete Element Method (DEM) is a family of numerical modeling techniques that are used to solve engineering problems that exhibit gross discontinuous mechanical behavior. For background on the DEM and several applications of the DEM other than transfer station modeling, the reader is referred to (Mustoe 1989 and Williams 1993). Hustrulid (1996) presents the first application of the DEM to modeling transfer stations. Nordell (1997) recently acknowledged the advantage of the DEM over traditional fluid mechanics models (Nordell 1994) for simulating transfer stations and has begun to use this modeling technique. Full disclosure of the numerical model used for the transfer point simulations in this paper can be found in Hustrulid (1997). While not containing information on the application of the discrete element method to transfer station design, Swinderman (1997) presents a comprehensive approach to design and maintenance issues of this critical conveyor component.

1. Overland Conveyor, Inc.

CONSTRUCTING A TRANSFER STATION SIMULATION

Setting up a discrete element simulation is different from other numerical modeling techniques. The system must be built up following Mother Nature's rules. The physical boundaries such as the steel chute and the rubber belt must be first defined. Once these are in place, the loading of material on the incoming belt can carefully begin. At this point, the user input is complete and Newton, with the help of a little computer science, takes over. The particles are checked with one another for contact, forces are applied following Hertzian contact equations, and finally the particle forces, velocities, and positions are updated with an explicit numerical method. This procedure continues until the simulation is complete. This section discusses the initial construction of the simulation.

Defining the Physical Boundaries

The first step in a discrete element simulation is the definition of the physical boundaries in the system. In the transfer station simulations, these boundaries include the steel structure, the head pulley, and the belts. The current implementation of the model handles planar and curved boundaries. Curved boundaries are required to correctly model the head pulley, curved chutes, and the fillet radius in the idler junction of the belt. Velocity profiles are defined for each of the boundaries to simulate the movement of the belt. In the current implementation, the boundaries are treated as rigid boundaries. This means that in the numerical simulation the belt will not mistrack from the forces acting on it. Drag from the skirts being pushed against the belt will also not be seen. This is not a limitation of the Discrete Element Method, only a feature that is not yet implemented. The planar and curved boundaries are defined in the model with the three-dimensional vertices of the boundaries. The boundaries of a typical transfer chute are shown in Figure 1.

Loading the Material on the Incoming Belt

In any discrete element simulation, one of the most critical aspects is the correct modeling of the initial conditions of the particles. When modeling transfer stations, the loading of the incoming belt must be carefully handled. During

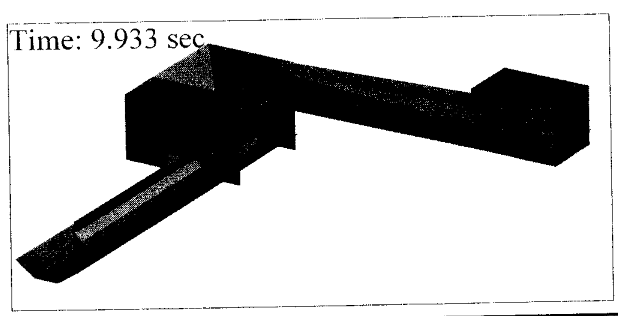

FIGURE 1 Transfer station boundaries

the development of this technology, several different methods of loading the incoming belt have been tried. This section presents the method that experience has shown to work the best and also discusses other methods that have been tried and either performed poorly or failed altogether.

The most reliable and successful is the use of a generation box in which particles with a given size distribution are randomly located and allowed to freely drop on the incoming belt. Friction forces between the material and the belt accelerate the material to the belt speed by the time it reaches the head pulley. Hustrulid (1996) uses this method of belt loading as shown in Figure 2.

The rate that material is created in the generation box is controlled by the desired tonnage on the belt and can be varied with time. This feature is particularly useful when modeling the starting or stopping of the conveyor belts. Using this method of loading produces a controllable, consistent, tonnage and size distribution on the belt.

The incoming belt can also be loaded by simulating a filled hopper that discharges material onto the incoming belt. The drawbacks to this method are listed below:

1. A significant number of extra particles must be modeled at the beginning of the simulation; thereby increasing the simulation time.
2. The flow rate on the incoming belt is difficult to consistently control - it varies with the depth of the hopper.
3. The size distribution of the particles on the incoming belt is determined by flow mechanics of the hopper.

This system of loading the belt is shown in Figure 3.

A method that falsely appears to work for short time duration is the loading of "slugs" of material on the belt. In this method, a slug of material, approximately 2 feet long, is loaded on the incoming belt, settled, and saved in a data structure. The velocity of the material in the slug is then set to the belt speed and allowed to move. Once the slug of material has moved the length of the slug, a second copy of the slug of material is loaded on the belt. The process continues, keeping a constant flow of material on the belt. The problem

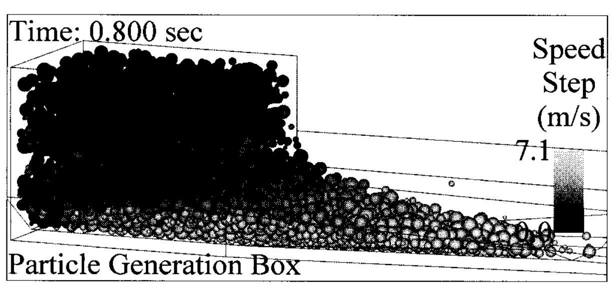

FIGURE 2 Particle generation box

experienced with this method is that, in practice, small pressure waves travel up and down the material on the belt. The adding of slugs of material to the belt introduces discontinuities in these waves that result in instabilities and massive pressure waves that are not realistic and produce incorrect results. In theoretical terms, this method of loading particles is attempting to use periodic boundaries without enforcing force and mass transfer at the boundaries. In practical terms, the locations and movements of the particles downstream influence the movements of the particles upstream. The net result is a phenomenon in the particles similar to the "water hammer" affect in fluids.

Similar "water hammer" problems are experienced when the model is divided into two parts in an attempt to shorten the required computer time. The logic behind this method is that the positions and velocities of the material coming off the incoming belt can be saved and removed from the simulation. In a second simulation, the particles are reinserted into the model and allowed to travel through the chute. The time savings come when several different chute configurations are run without having to re-model the material traveling on the incoming belt. Nordell (1997) uses this method. In practice, the time savings is almost insignificant because during the initial loading period, with no particles in the chute or on the second belt, the simulations run relatively quick. The "fatal flaw" of this method is that while maintaining the mass transfer at the extraction/insertion point, or "particle bucket," the method ignores the force transfer at this boundary. This shortcut causes major instabilities in the modeling results, particularly at higher tonnage.

Particle Size and Shape Considerations

The framework of the DEM allows for particles and boundaries to be of any size and shape. It also allows for the inclusion of fluid or gas interaction of the particles. Research has been completed on the use of ellipses, superquadrics, clumped particles, and general shaped particles in two and three dimensions. The current limitation is the required computer time for these simulations.

The simulations presented in this paper using spheres and clumps of spheres require approximately 8-12 hours of computer time on a dual processor 200 MHz Pentium Pro. Using more complicated elements such as ellipses or superquadrics can increase the simulation time by orders of magnitude.

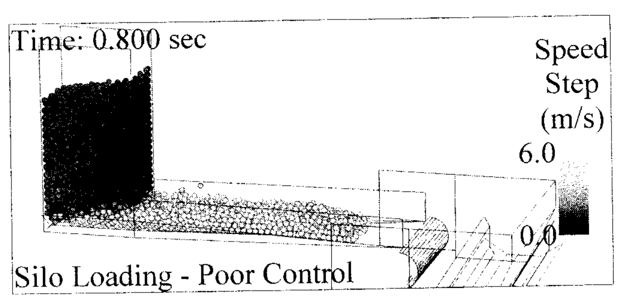

FIGURE 3 Hopper belt loading

Hustrulid (1997) shows there is even a severe time penalty associated with just increasing the range of the size distribution of spheres in a simulation.

CONFIRMING THE RESULTS OF A DEM SIMULATION

With any numerical modeling technique, it is important to verify the accuracy of the results of the model. With the Discrete Element Method, there are several approaches used to build confidence in the computer program.

The first method is a verification of the micro-mechanics of the program. This process involves bouncing individual particles off each other and boundaries then comparing their response with exact solutions.

The kinetic and potential energy of the system is important to monitor. After filling a silo with particles, the kinetic energy of the system should approach zero. If a constant, nonzero, kinetic energy is reached, there may be trouble with the friction model being used. Erratic variation of the kinetic and potential energy is an indication that the time step in the numerical integration scheme is too large and the system is unstable.

Checking the macro-mechanics of the system is more difficult. Several checks of the expected behavior in transfer stations have been developed. Verifying that the tonnage exiting the system is equal to the tonnage being loaded on the incoming belt is an obvious first check. A second measurement that can be obtained from the DEM results is the force required to accelerate the material on the second belt. This measurement can be compared with the acceleration force predicted by CEMA (1988). Hustrulid (1996) presents both of these checks. Checking the vertical force on the second belt has also increased the confidence in the computer implementation. The expected vertical force on the belt is calculated as

$$F_v = \frac{Q}{V} \qquad \text{(EQ 1)}$$

where Q is the tonnage in tons/hr and V is the belt speed in meters/second. Figure 4 shows the vertical force on the lower belt shown in Figure 1. Carrying 1,633 tonne/hr and traveling 3.15 m/sec the vertical force should be 144 kg/m.

In region A, prior to the chute, there is no material on the belt. In region B, under the chute itself, the material is impacting the belt and there is a slight build up increasing the weight on the belt. In region C, the 45-degree angle of the skirts is carrying some of the material load. At point D, the vertical force rises slightly as the material falls off the skirts onto the belt. In region E, the vertical force is exactly equal to its expected value.

MEASUREMENTS USED TO IMPROVE TRANSFER STATION PERFORMANCE

In a discrete element method, the motion of each body or particle is calculated each time step. To calculate this motion, the location, velocity, and forces acting on each particle must also be calculated each time step. With a time step of 10^{-5} seconds, an enormous amount of data can be generated.

To better understand and use all this data, several techniques are employed. The most intuitive technique is scientific visualization using animated 3-dimensional simulation of the DEM data. These visual representations of the data allow the engineer to see the material flow. Colors representing the speed of the material or other values such as pressure can be applied to present an added dimension to the simulation. The shortcoming of these visualizations is that it is difficult to quantify if one design is better or worse than another.

To overcome this shortcoming, simple graphing techniques are used. Initially, data that can be compared with traditional hand calculations is plotted to build confidence in the model. In the transfer point simulation, the material flow rate, the force to accelerate the material and the vertical force on the belt are plotted and compared to expected values.

These plots can be used to compare different transfer point designs but do not answer the question of which design is better. To answer this question, the DEM data is used to calculate values more applicable to the problem of designing a better transfer station. Most significantly, an expected belt wear profile is calculated based on the traditional method of predicting abrasive wear. To measure how well the load is centered on the receiving belt, the moment arm to the center of mass is calculated. The center of mass of the material on the belt will effect the belt tracking. The lateral force on the belt also influences the tracking of the belt and is measured.

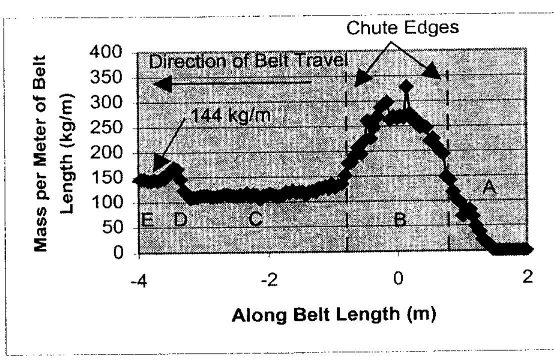

FIGURE 4 Vertical force on receiving belt

Three Dimensional Visualization of Results

Plotting and animating the results of the discrete element simulations can answer several questions. The influence of rock boxes in tripper applications can be seen in Figure 5.

The discrete element simulations can also be used to correctly locate complicated chute geometry such as the conical chute shown in Figure 6.

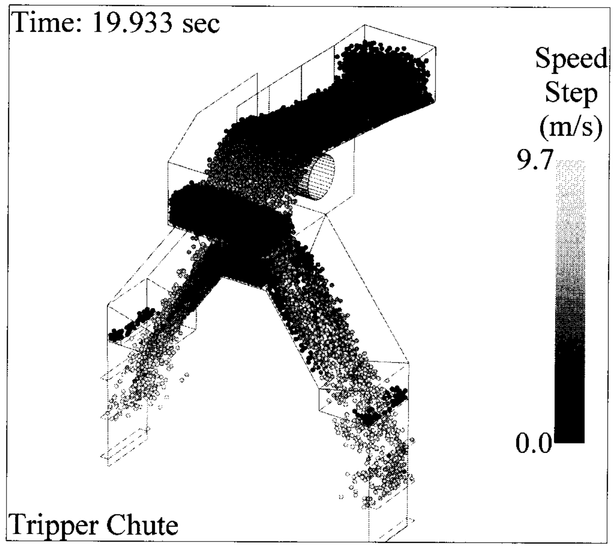

FIGURE 5 Tripper chute simulation

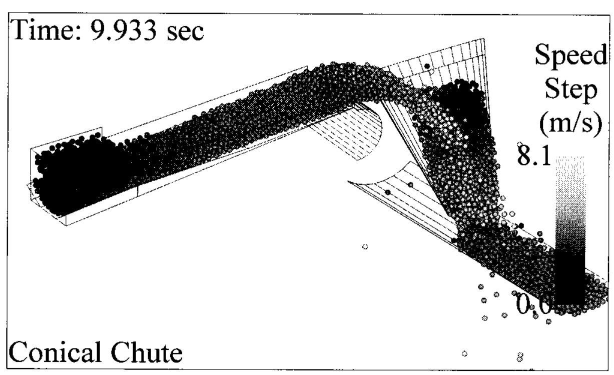

FIGURE 6 Conical chute

In the conical chute simulation there were no skirt boards modeled on the receiving belt to see how much material would remain on the belt without them.

When increasing the tonnage on a system or installing a new system, the discrete element simulations can be used to determine if the transfer stations can handle the tonnage as shown in Figure 7.

The DEM can then be used to figure out what changes need to be done to make the chute work as shown in Figure 8.

Wear Occurring in Transfer Stations

This section looks at the wear occurring in transfer stations. The steel plates making up the chute structure can be treated separately from the wear occurring to the belt. This section focuses on the wear occurring to the belt but is equally applicable to the chute structure.

In most transfer stations, four areas that may be causing the belt to wear can be identified: (1) wear between the skirts and the belting, (2) material trapped between the skirts and the belting, (3) cover damage resulting from material

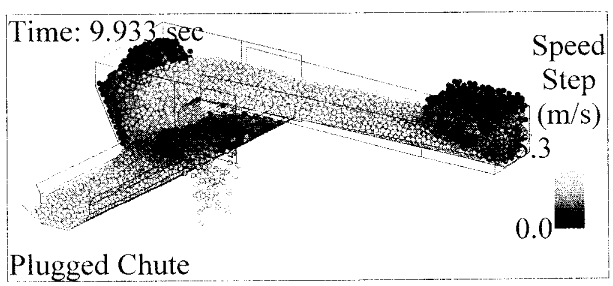

FIGURE 7 Plugged chute

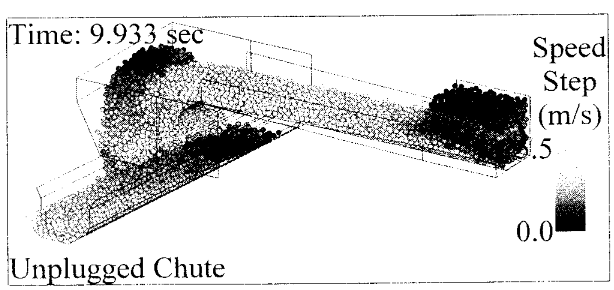

FIGURE 8 Unplugged chute

impacting the belt at high speeds, and (4) wear from the turbulence of bringing the material up to the belt speed. Any or all four of these situations may attribute to belt wear.

An indication of the type of wear occurring is seen in the cover wear profile. Accurate wear profiles can be measured at specific locations with ultrasonic probes for fabric belts and linear output proximity probes for steel cable belts. Using lasers mounted across the belt width, it may be possible to measure the wear profile for the entire belt length. These tests can be performed in situ. Identifying the areas of the belt that are wearing provides an indication of the mechanism causing the wear such as material turbulence, skirt-belt contact, or other causes.

In this section, the cause, evidence, and general remedies of each type of wear listed above are discussed. Each of the possible causes are presented on an individual basis; however, it is important to realize that any combination of these may be present and result in the belt wear. A method for quantifying belt wear with a discrete element simulation is also presented.

Wear Between the Skirts and the Belting. The material carried on the belt will push the rubber skirts against the belt. This will cause wear. If the rubber skirts are softer than the belt cover, they will be sacrificed and will need to be replaced often. If the skirts are harder than the belt cover, the belt cover will wear. This mechanism of wear is shown in Figure 9. Wear between the belt and the skirts will be worse if material is trapped between them. Wear from trapped material is discussed in the next section.

If this type of wear is occurring, the skirts should wear out relatively quickly on the side contacting the belt. If the skirts are not being sacrificed, then the belt cover is worn away. The wear profile expected from this wear mechanism is shown in Figure 10.

The approximate distance between the wear points labeled as “a” is the calculated distance between the inside edges of the rubber skirts. The total belt width is labeled as “b.”

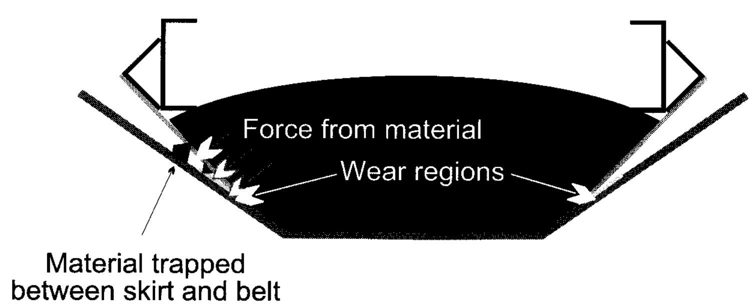

FIGURE 9 Belt wear resulting from skirting contact

The solutions to this type of wear are straightforward:

- Change to a different skirt board configuration. This will result in less wear but may lead to more material leakage from the transfer station.
- Change to a softer rubber compound for the rubber skirt. The skirt would be sacrificial and have to be replaced more often.
- Change to a more abrasive resistant belt cover. This may be undesirable from other aspects in the conveyor system.

Wear From Material Trapped Between the Skirts and the Belting. Wear between the skirts and the belt will be worse if material gets trapped between the two.

If material is getting trapped between the skirts and the belt, it should wear only that side of the belt. The expected wear profile is shown in Figure 12.

The solutions to this type of wear are straightforward:

- Better seal the transfer chute so the material cannot become trapped.

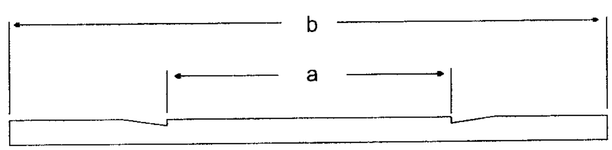

FIGURE 10 Expected wear profile from skirting contact

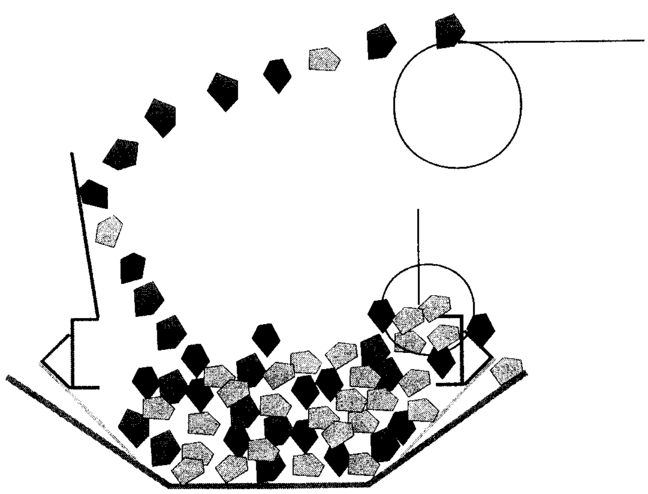

FIGURE 11 Sealing inside the transfer chute

- Change the skirt design to one that is less likely to trap material between the skirt and the belt.

Cover Damage From Material Impacting the Belt. In some transfer stations, the material hits the belt at high velocity. The energy of the material is not being redirected or removed by the transfer geometry as it should in these cases. The belt covers are absorbing the energy that may cause increased wear. If the impact bed is very solid, it increases the possibility of damage to the belt. This wear mechanism is shown in Figure 13.

If this type of cover damage is occurring, the wear should be nonuniform between the skirts. An approximated wear profile is shown in Figure 14.

The solutions to this type of cover wear are not simple. They will require some redesign of the transfer station. The possible remedies are listed below:

- Modifying the transfer geometry to reduce the impact forces. How to change the geometry can be determined via trial and error or by using a discrete element model as presented in the next major section.

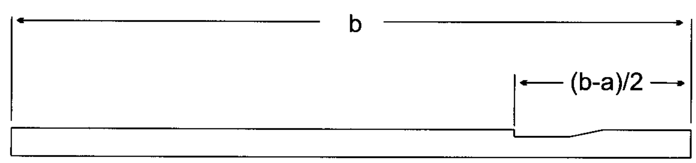

FIGURE 12 Expected wear from the material trapped between the skirt and the belt

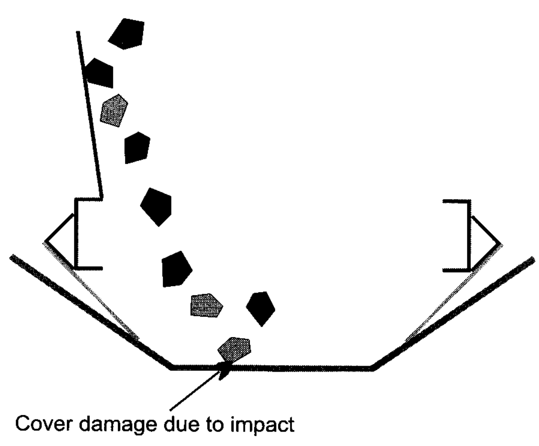

FIGURE 13 Impact damage

- Change to a gentler style impact bed that will cushion the impact some. This solution attempts to deal with the problem instead of minimizing the cause.

Note: Changing to a different type of skirt configuration will expose more belt in the transfer point area. If impact damage is occurring, changing the skirt design may make this wear mechanism more prevalent.

Wear From the Turbulence of Accelerating the Material up to the Belt Speed. The material being loaded onto the belt must be accelerated up to the belt speed. This acceleration requires a force between the material and belt cover. The material can be turbulent until it reaches the belt speed at which point it quiets down. This turbulence may lead to belt wear. Ideally the material would be gently placed, fines first, already up to speed on the receiving belt. In some transfer stations, the material impacts the belt at a high downward speed. Turbulence is then created from the high downward impact speed of the material. After the material has a chance to settle down, it is then accelerated to the speed of the belt.

In the skirt configuration shown in Figure 15, there is a lot of static area the material is in contact with. The static area increases the distance required to accelerate the material up to belt speed. High material impact velocity and high contact surface area with the skirts lead to a lengthened turbulent zone. This lengthened turbulent zone causes increased belt wear.

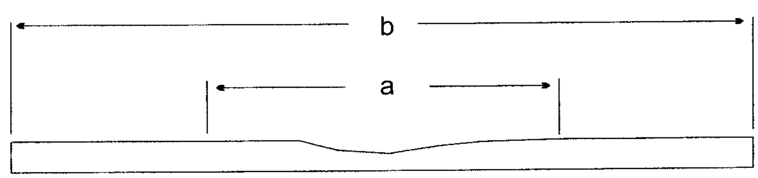

FIGURE 14 Approximate wear profile resulting from material impact damage

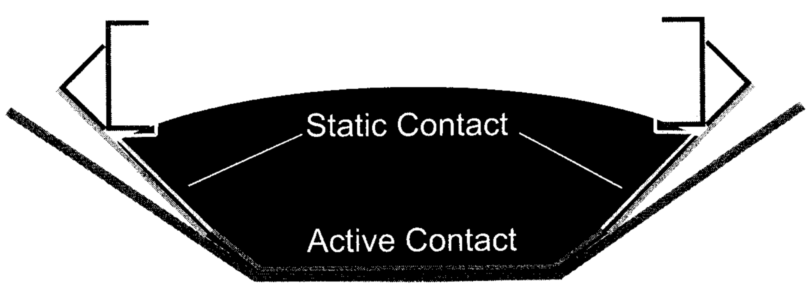

FIGURE 15 Skirt contact area

If this type of wear is occurring, the belt should be worn pretty uniformly in the center between where the skirts make contact with the belt. An expected wear profile is shown in Figure 16. The wear on the inside of the rubber skirts from the material is also expected to be high.

There are several solutions that reduce this type of wear:

- Change the skirt design so that more belting and less skirting is in contact with the material. This will result in less wear but may lead to more material leakage from the transfer station. Changing the skirt design may also increase the wear from material impacting the belt.
- Modify the transfer point geometry to place the material on the belt in a more ideal fashion.

Other Possible Causes of Wear. Belt wear that is not associated with the load point can result from rough or misaligned return idlers and from the material shifting as is passes over each carry idler. The wear from the material shifting will occur in areas with high belt sag.

Calculating Wear With the DEM. Several types of wear are defined in the literature including adhesive, abrasive, surface fatigue, and oxidation wear. "Abrasive wear mechanisms are generally considered to be any mechanism by which the hard aspirates or particles cause damage in a single action." (Bayer, 1994) An erosion wear process can be treated as a special type of abrasive wear. It is believed that the abrasive wear mechanism is the typical type of wear occurring in transfer stations.

The methodology that has been developed to calculate the abrasive wear with the DEM model is based on general derivations by Finnie (1958, 1978) and more specifically Bayer (1994). Several of the generalizations made by Bayer and Finnie concerning the path of the abrading material are not needed because the material contact paths are known in the DEM model.

The volume of material worn away through abrasive wear is calculated by considering the amount of material removed by an individual hard particle or asperity sliding against and gouging material out of a softer material such as the conveyor cover. The material abraded away during the impact of a hard particle on a softer surface is shown in Figure 17. In this model, it is assumed that plastic deformation occurs during the entire contact process.

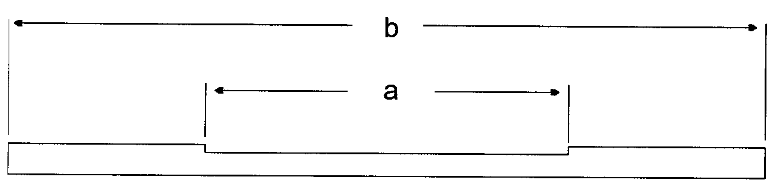

FIGURE 16 Expected wear profile from material turbulence

In the DEM, the paths of every impacting particle is implicitly modeled and can be used to directly predict the expected wear. Figure 18 shows the volume of material assumed to be removed at one contact during one time step. The body moves from the position at time = t to the position time = t + 1 as shown in Figure 18.

The volume of the removed material is calculated as

$$Volume = VRS \cdot \Delta t \cdot Ax \qquad \text{(EQ 2)}$$

where
VRS = the relative velocity in the shear direction at the point of contact

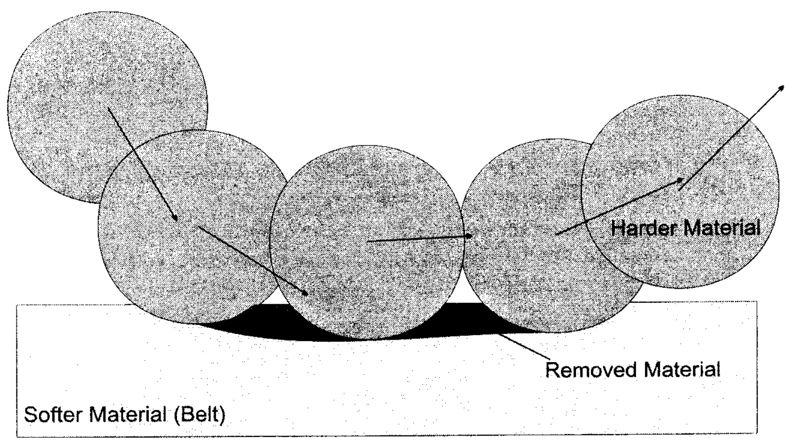

FIGURE 17 Contact path

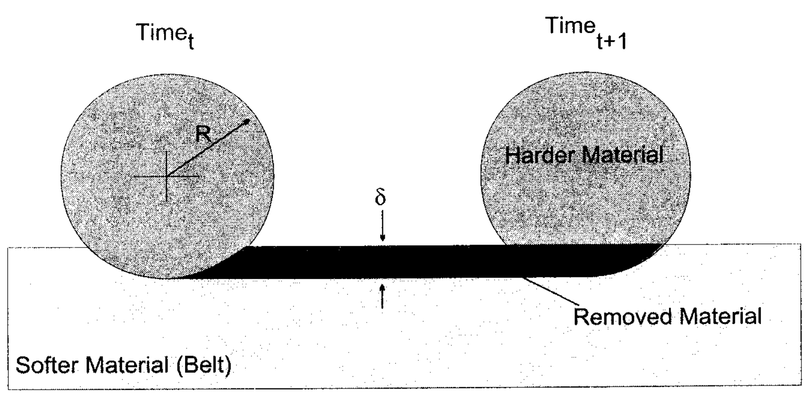

FIGURE 18 Abrasive wear model

Δt = the time step used in the simulation
Ax = cross sectional area of the particle

The cross-sectional area, Ax, for a spherical shape in contact with a plane is shown in Figure 19.

The cross-sectional area of the contact area is calculated as follows:

$$Ax = R^2\left(\theta - \frac{\sin 2\theta}{2}\right) \quad \textbf{(EQ 3)}$$

where the angle, θ, can be found using

$$R - \delta = R\cos\theta \quad \textbf{(EQ 4)}$$

Since θ is expected to be small, the first two terms of the MacLaurin's Formula for sine and cosine

$$\sin\theta = \frac{\theta}{1!} - \frac{\theta^3}{3!} + \frac{\theta^5}{5!} - \frac{\theta^7}{7!} + \ldots \quad \textbf{(EQ 5)}$$

$$\cos\theta = 1 - \frac{\theta^2}{2!} + \frac{\theta^4}{4!} - \frac{\theta^6}{6!} + \ldots \quad \textbf{(EQ 6)}$$

are used to solve for the area as a function of δ. The resulting equation is

$$Ax = R^{0.5}\delta^{1.5} \cdot 1.8856 \quad \textbf{(EQ 7)}$$

In the derivation of the amount of wear by Bayer (1994), he assumes that the particle has a conical shape as shown in Figure 20.

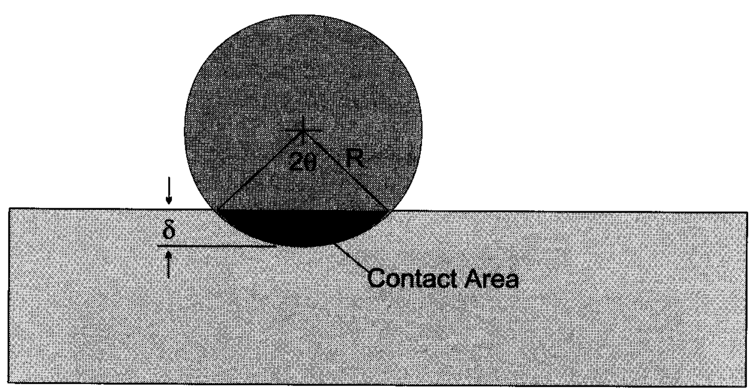

FIGURE 19 Cross-sectional contact area of a sphere

The cross-sectional area for this shape is

$$Ax = \delta^2 \tan \alpha \qquad \textbf{(EQ 8)}$$

where tan (α) is treated as the sharpness of the particle.

In the current discrete element model, clumped spheres are being used to model the material. With the sphere, the cross-sectional area is proportional to the 3/2 power of the penetration. With the cone, the cross-sectional area is proportional to the square of the penetration. Since the square of a number is computationally faster for the computer to perform, the equation for the cross section of a conical asperity is chosen for implementation. Also, since at this point only comparisons of the relative wear between different transfer station geometries are being looked at, the sharpness factor of the particle, tan (α), is just a scaling factor. At this stage, it will be simple set equal to 1.

In this case, the wear volume equation becomes

$$Volume = VRS \cdot \Delta t \cdot \delta^2 \cdot \tan \alpha \qquad \textbf{(EQ 9)}$$

The wear model presented has been shown to be most valid for ductile materials and less valid for brittle materials. The use of the DEM model is acceptable since the rubber covers for the conveyor belt are considered to be ductile. The model also assumes that plastic deformation is occurring during all contacts. This is something that can be refined in the future but for now it will produce conservative results.

Two graphs depicting the "wear profiles" of the belt are created. The units of the wear are reported as $K\frac{m^3}{m \sec}$. This is the volume of wear occurring in one second per meter of belt length or belt width. The area under the curve is the total volume of wear occurring during one second. These values are reported as a scalar multiple, K, of the true volume wear occurring. This K is unknown but will be constant if the model parameters are held constant. Full tonnage on the belts is used to generate the wear profile graphs.

In Figure 21, the dashed vertical lines indicate where the edges of the skirting meet with the belt. In the wear profile in Figure 21, two patterns can be seen.

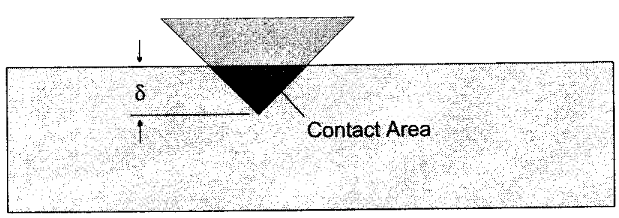

FIGURE 20 Cross sectional contact area of conical asperity

First, there is a significant dip at 0.4 meters and a smaller dip at 0.81 meters. The dips in the wear profile at these locations are attributed to the concave angle at the idler junctions. The lower belt has been modeled as three planes and results in a concave angle at their junction as shown in Figure 22. This results with particles being in contact with two of the planes when they are in this region. Of these two contacts, the areas at 16.5 inches and 31.5 inches take the higher loads. This can be seen in the wear profile. Modeling the idler junction with a fillet that has a radius slightly larger than that of the largest particle helps reduce this affect. The fillet ensures each particle is in contact with the belt at only one location.

The second pattern is the overall roughness of the wear profile in Figure 21. The wear profile was generated from one second of simulation time with the belt running at full tonnage. Generating the wear profile over a longer simulation time will tend to smooth out the profile.

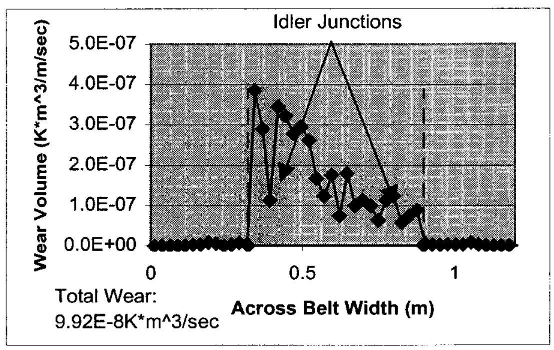

FIGURE 21 Wear profile across the width of the belt

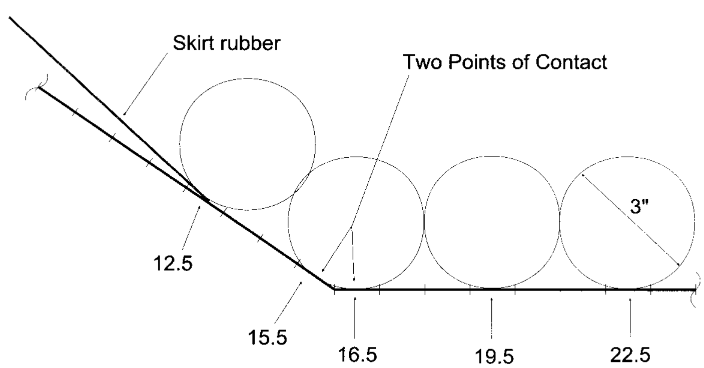

FIGURE 22 Possible arrangement of bodies on receiving belt

Figure 23 shows the wear profile along the length of the belt. In contrast to Figure 21, which shows the area of the belt that would wear out, Figure 23 shows where in the transfer station the wear is occurring. The area under the wear curves in Figure 21 and Figure 23 is a measure of the total volume of material worn and they are equal.

In Figure 23, the vertical dashed lines are at the edges of the transfer point at -0.78 meters and 0.78 meters and the incoming belt is centered at 0 meters.

Lateral Force on the Belt

The lateral force on the belt is the amount of force that the material puts on the belt that would tend to make the belt mistrack. In Figure 24, the lateral force acting on the belt is shown. The dashed vertical lines represent the sides of the transfer point and the incoming belt is centered at 0 meters. The direction of the force on the belt is clarified in Figure 25.

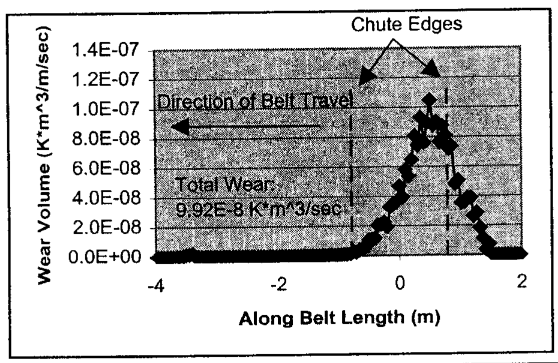

FIGURE 23 Wear profile along the length of the belt

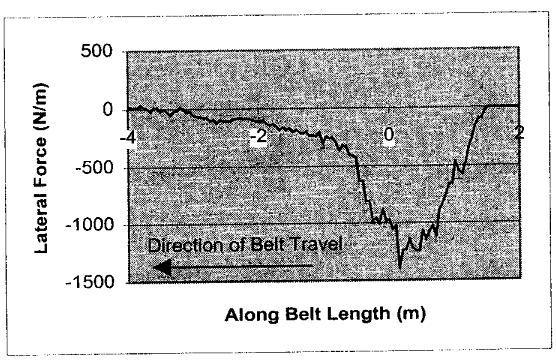

FIGURE 24 Lateral force on the belt

Ideally, the lateral force would equal zero; however, in a 90° transfer station this may not be possible. The lateral force, in combination with belt tension, will effect how much the belt will tend to mistrack at the transfer station.

Moment Arm

Another influence on the tendency of the belt to mistrack is how well the belt is centrally loaded. This can be measured by calculating the moment arm of the forces acting in the vertical direction. Figure 26 shows the calculated moment along the belt length at the transfer station.

The "spikes" in the moment arm curve at approximately 1.5 meters are results of the division of very small numbers. These small numbers are from the mass of the material on the belt being close to zero in this region. These spikes can

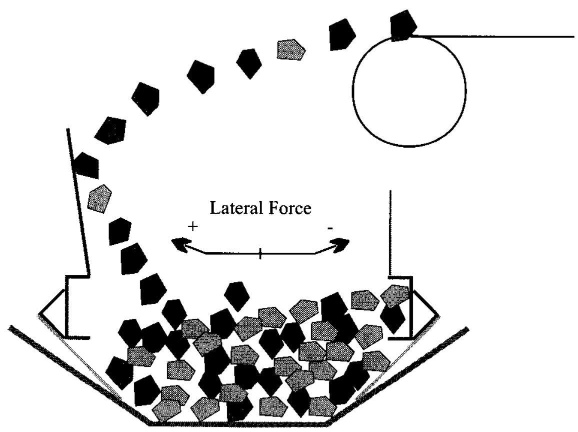

FIGURE 25 Direction of the lateral force on the belt

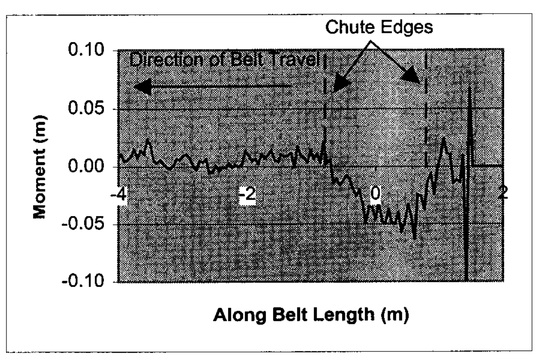

FIGURE 26 Moment arm of the center of material

be safely ignored. The direction of the moment arm of the center of material on the belt is illustrated in Figure 27.

In the current DEM implementation, the belt is considered to be rigid and does not mistrack as a result of the off-centered load or in response to lateral forces on the belt. Intuitively, a positive moment arm should work against a negative lateral force on the belt. The combination of these two influences would give an overall impact on the belt tracking.

CONCLUSION

The discrete element method has been shown to be an excellent computational tool for simulating the material flow in transfer stations. Three-dimensional visualizations of the modeling results provide an overall feel of the flow behavior in the chute. Wear profile, moment arm, and lateral force diagrams provide the engineer with a definable means of improving transfer station design.

REFERENCES

Bayer, R.G., 1994, *Mechanical Wear Prediction and Prevention*, Marcel Dekker, New York.

CEMA, 1988, *Belt Conveyors for Bulk Materials*, Conveyor Equipment Manufacturers Association, Third Edition.

Finnie, I., 1978, "Erosion of Surfaces by Solid Particles," *Source Book on Wear Control and Technology*, American Society for Metals.

Finnie, I., 1958, "The Mechanism of Erosion of Ductile Metals," *Proceedings of the Third U.S. National Congress of Applied Mechanics*, The American Society of Mechanical Engineers.

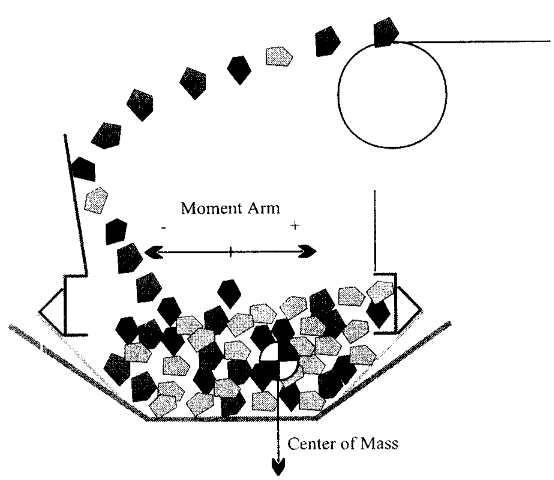

FIGURE 27 Direction of the moment arm

Hustrulid, A.I. and Mustoe, G.G.W., 1996, "Engineering Analysis of Transfer Points Using Discrete Element Analysis," *Bulk Material Handling by Conveyor Belt*, SME.

Hustrulid, A.I., 1997, *A Computational Methodology for Modeling Large Scale Sublevel Caving with a Three-Dimensional Discrete Element Method*, PhD Dissertation, Colorado School of Mines, Golden, Colorado.

Mustoe, G.G.W., et al., 1989, *Proceedings*, First U.S. Conference on Discrete Element Methods, Golden, Colorado, August.

Nordell, L.K., 1994, "Palabora Installs Curved Transfer Chute in Hard Rock to Minimize Belt Cover Wear," *Bulk Solids Handling*, Vol. 14, No. 4, October/December, pp. 739-743.

Nordell, L.K., 1997, "Particle Flow Modeling: Transfer Chutes & Other Applications," BELTCON 9, South Africa, October 22-24.

Swinderman, R.T., et al., 1993, *Foundations2, The Pyramid Approach to Control Dust and Spillage From Belt Conveyors*, Martin Engineering, Illinois.

Williams, J.R. and Mustoe, G.G.W., 1993, *Proceedings*, Second International Conference on Discrete Element Methods (DEM), The Massachusetts Institute of Technology, March 18-19.